JOURNAL OF AGRICULTURAL AND FOOD CHEMISTRY

pubs.acs.org/JAFC Article

Assessment of the Conformation Stability and Glycosylation Heterogeneity of Lactoferrin by Native Mass Spectrometry

Yu Mu,[▽] Shan Zhao,[▽] Jing Liu, Zheyi Liu, Jian He, Hongfang Cao, Heng Zhao, Caiyun Wang, Yan Jin,* Yanxia Qi,* and Fangjun Wang*

Cite This: J. Agric. Food Chem. 2024, 72, 10089−10096 Read Online

ACCESS | Metrics & More | Article Recommendations | Supporting Information

ABSTRACT: Lactoferrin (LTF) has diverse biological activities and is widely used in functional foods and active additives. Nevertheless, evaluating the proteoform heterogeneity, conformational stability, and activity of LTF remains challenging during its production and storage processes. In this study, we describe the implementation of native mass spectrometry (nMS), glycoproteomics, and an antimicrobial activity assay to assess the quality of LTF. We systematically characterize the purity, glycosylation heterogeneity, conformation, and thermal stability of LTF samples from different sources and transient high-temperature treatments by using nMS and glycoproteomics. Meanwhile, the nMS peak intensity and antimicrobial activity of LTF samples after heat treatment decreased significantly, and the two values were positively correlated. The nMS results provide essential molecular insights into the conformational stability and glycosylation heterogeneity of different LTF samples. Our results underscore the great potential of nMS for LTF quality control and activity evaluation in industrial production.

KEYWORDS: *native mass spectrometry, lactoferrin, conformation stability, glycosylation heterogeneity, heat treatment*

1. INTRODUCTION

Lactoferrin (LTF), a member of the transferrin family, is a multifunctional glycoprotein with a molecular weight (MW) of approximately 80 kDa.[1] LTF can be found in many biological secretions of mammals, such as milk, colostrum, tears, saliva, semen, and plasma.[2,3] Moreover, it possesses many biological activities, including antimicrobial, anti-inflammatory, antiviral, and antitumor properties.[4−8] Commercialized LTF is primarily derived from bovine milk and is incorporated into a range of functional foods, including infant formula, nutritional supplements, and dairy products.[9−11]

Glycosylation is one of the most common post-translational modifications (PTMs) and is crucial to the biological activity of proteins, including immunogenicity, antigenicity, and resistance to protein hydrolysis.[12] All LTFs identified so far are glycosylated with significant heterogeneity in both glycosylation sites and occupancy.[13] The LTF glycosylation state and glycan composition are dependent on the milk source, while its conformation is greatly influenced by industrial processing processes such as heat treatment.[14] Heat treatment will induce LTF structure unfolding, mainly including the α-helix loss and β-sheet increase, resulting in the increase of protein surface hydrophobicity[15] and the decrease of its biological activity.[16] Sodium dodecyl sulfate-polyacrylamide gel electrophoresis (SDS-PAGE)[17] and liquid chromatography (LC) are common techniques utilized for the quality control of LTF production.[18] However, these quality control methods mainly provide the purity criteria. In brief, the narrow linear range and high variability of SDS-PAGE limit its usage;[19] reversed-phase LC (RPLC)[20−22] is commonly applied for product purity detection, while size exclusion chromatography (SEC)[23] can be utilized for product purity and MW determination. All of these quality control strategies cannot provide molecular insights into LTF glycosylation heterogeneity and conformation stability. Therefore, there is an urgent need to develop a quality control method to accurately assess the glycosylation heterogeneity and conformation stability of LTF at the molecular level. In recent years, native mass spectrometry (nMS) based on nondenaturing electrospray ionization (nESI) has emerged as a powerful tool for exploring protein high-order structures and interactions.[24−28] nESI transfers intact proteins from solution to the MS gas phase, preserving their compact structures and noncovalent interactions.[29,30] nMS has been widely utilized to characterize protein conformation stability, subunit assembly, and protein−ligand interactions.[31−35] The application of nMS successfully elucidated the dynamic conformation and glycosylation heterogeneity of therapeutic monoclonal antibodies (mAbs) with multiple glycosylations.[36] Furthermore, nMS was also applied to compare the conformation similarity and distinguish the glycosylation difference of fetuin proteins from different sources.[37]

In this study, we established an nMS strategy to characterize the conformation and glycosylation heterogeneity of LTF (Figure 1). LTF from different sources and under transient high-temperature treatments could be assessed and differentiated by nMS and glycoproteomic analysis. The molecular

Received: November 26, 2023
Revised: April 1, 2024
Accepted: April 4, 2024
Published: April 16, 2024

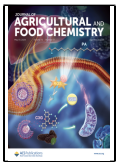

https://doi.org/10.1021/acs.jafc.3c08860
J. Agric. Food Chem. 2024, 72, 10089−10096

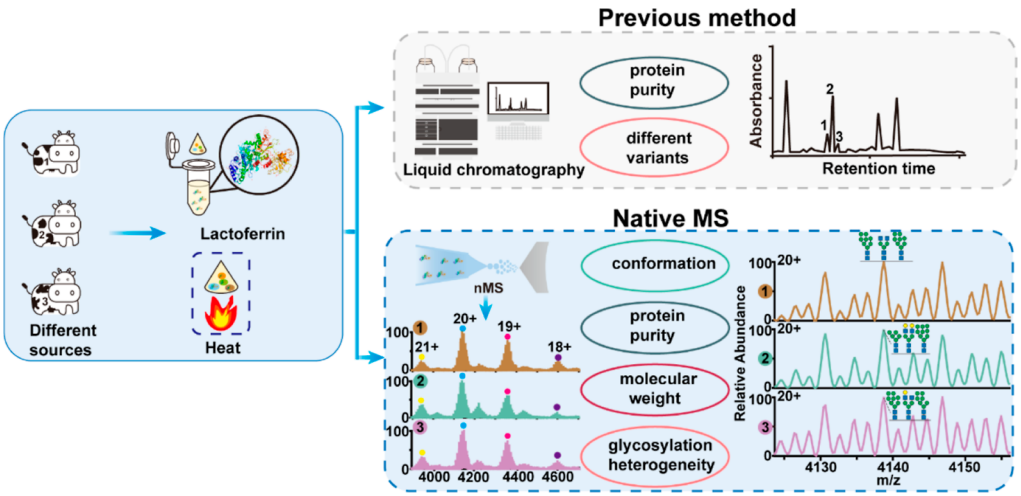

Figure 1. Schematic diagram of the nMS characterization of the conformation stability and glycosylation heterogeneity of LTF.

insights into conformation stability and N-glycan of LTF samples were related to their antimicrobial activity. LTF samples with a narrow charge distribution and relatively high peak intensity in nMS spectra exhibited higher antimicrobial activity due to their more stable active conformations.

2. MATERIALS AND METHODS

2.1. Materials and Reagents. Bovine LTF samples were obtained from Inner Mongolia Yili Co. Ltd. (Hohhot, China), which were labeled as LTF1, LTF2, and LTF3. *Escherichia coli* (*E. coli*, CICC10899) was purchased from the China Center of Industrial Culture Collection. Agar powder was acquired from Beijing Solaibao Technology (Beijing, China). Luria−Bertani (LB) broth was purchased from Hangzhou Microbial Reagent Co., Ltd. (Hangzhou, China). The borosilicate glass capillary was from Sutter Instruments Co. Ltd. (California, USA). All other chemicals were purchased from Aladdin Biochemical Technology Co. Ltd. (Shanghai, China).

2.2. Sample Preparation. For nondenaturing sample preparation, 10 μM LTF solution was prepared using ammonium acetate solution (pH = 7.08). The solution used in nESI requires not only volatility but also sufficient ionic strength to maintain the native conformation of protein.[38] We optimized the concentration of ammonium acetate solution, and 200 mM was utilized for nMS analysis of LTF. In heat treatment experiments, the LTF solution was heated at 72 °C for 15 s or 100 °C for 10 s. The LTF solution was desalted in 10 kDa ultrafiltration tubes and centrifuged at 14,000*g* for 10 min before nMS analysis. For comparison, the denatured samples were prepared in an aqueous solution with 50% methanol and 1% formic acid (FA).

2.3. Protein Digestion and Glycopeptide Enrichment. Three LTF samples were dissolved in 20 mM NH_4HCO_3 buffer and denatured by incubation in a water bath at 95 °C for 3 min. After reduction with 5 mM tris(2-carboxyethyl)phosphine (TCEP) at 25 °C for 30 min, alkylation was performed with 10 mM iodoacetic acid (IAA) for 30 min in the dark at 25 °C. Then, chymotrypsin was added at a ratio of 1:50 (enzyme/protein, w/w), and the mixture was incubated overnight at 30 °C for protein digestion. After adjusting the pH to 3.0 by using 10% FA, the protein digest was lyophilized. For glycopeptide enrichment, 40 μg of the digested peptides was redissolved into 300 μL of loading buffer (CH_3OH/H_2O/ACN/TFA = 15:5:79:1, v/v/v/v) and mixed with the "click maltose" hydrophilic interaction liquid chromatography (HILIC) material[39] at a ratio of 1:50 (w/w), followed by shaking for 10 min.[40] After centrifugation at 14,000*g* for 3 min, the supernatant was removed, and the HILIC material was washed twice with 200 μL of loading buffer. Finally, the enriched glycopeptides were eluted from the HILIC material by using 80 μL of elution buffer (H_2O/ACN/TFA = 70:30:0.1, v/v/v), lyophilized, and stored at −80 °C for further usage.

2.4. LC−MS/MS Analysis and Data Processing. The lyophilized glycopeptides were redissolved into 0.1% FA solution at 0.1 mg/mL. High-performance LC (HPLC) with tandem spectrometry (LC−MS/MS) analysis was performed on an Orbitrap Fusion Lumos Tribrid mass spectrometer equipped with a nanospray ion source and a Vanquish Flex HPLC system (Thermo Fisher Scientific). In brief, the enriched glycopeptides were first injected onto a 3 cm × 150 μm i.d. trap column (C18, 3 μm), followed by separation on a 15 cm × 75 μm i.d. capillary column (C18, 2.4 μm). The 0.1% (v/v) FA aqueous solution and 0.1% FA/80% ACN were utilized as mobile phases A and B, respectively. The flow rate was set to about 250 nL/min. The reversed-phase binary separation gradient was 6−35% mobile phase B in 50 min. The full mass scan range was acquired from 350 to 1800 m/z, with a mass resolution of 120,000. The data-dependent acquisition (DDA) mode was employed, where the top 20 precursors were subjected to MS/MS analysis at a resolution of 30,000. For the MS/MS measurements, both higher-energy collision dissociation (HCD) and electron transfer combined with higher-energy collision dissociation (EThcD) were used and performed with normalized collision energies of 28 and 15%, respectively. The maximum injection time was set to 100 ms. The acquired raw files were processed by pGlyco 3.0 software (https://github.com/pFindStudio/pGlyco3) for the interpretation of intact N-glycopeptide spectra.[41] The FastaNGlysiteN2J.exe program was used to convert the bovine LTF database (https://www.uniprot.org/) file format into N2J format, and the pGlyco3GUI.exe program was used to retrieve mass spectral data sets in the bovine LTF database. The parameters for database retrieval were fragmentation mode HCD + EThcD, enzyme name chymotrypsin, digest C-Term FYWML, maximum miss cleavage 5, glycopeptide FDR cutoff 0.01, precursor tolerance 10 ppm, and fragment tolerance 20 ppm, all default values of pGlyco3.0 software. Then, the gLabel.exe program was used to retrieve the mascot generic format (MGF) files to obtain the secondary mass spectra of N-glycans. The glycopeptides identified at least 2 times in 3 replicate experiments with a default score value > 0.5 were considered reliable results.

2.5. nMS Analysis. The nMS experiments were performed on an Exactive Plus Orbitrap instrument with an extended mass range (EMR) (Thermo Fisher Scientific). The MS parameters were set as follows: mass scan range 1000−7000 m/z with 17,500 mass resolution, in-source CID 30.0 eV, CE 10.0, AGC target 5×10^5, maximum inject time 100 ms, nESI voltage 0.8−1.5 kV, source DC offset 25, injection DC 9, inter lens 8, bent DC 7, transfer multipole DC tune 0, C-trap entrance lens tune offset 2, EMR mode on, and trapping gas pressure setting 2. The inner tip diameter of the static nanoelectrospray emitter was 600 nm, made from a borosilicate glass

https://doi.org/10.1021/acs.jafc.3c08860
J. Agric. Food Chem. 2024, 72, 10089−10096

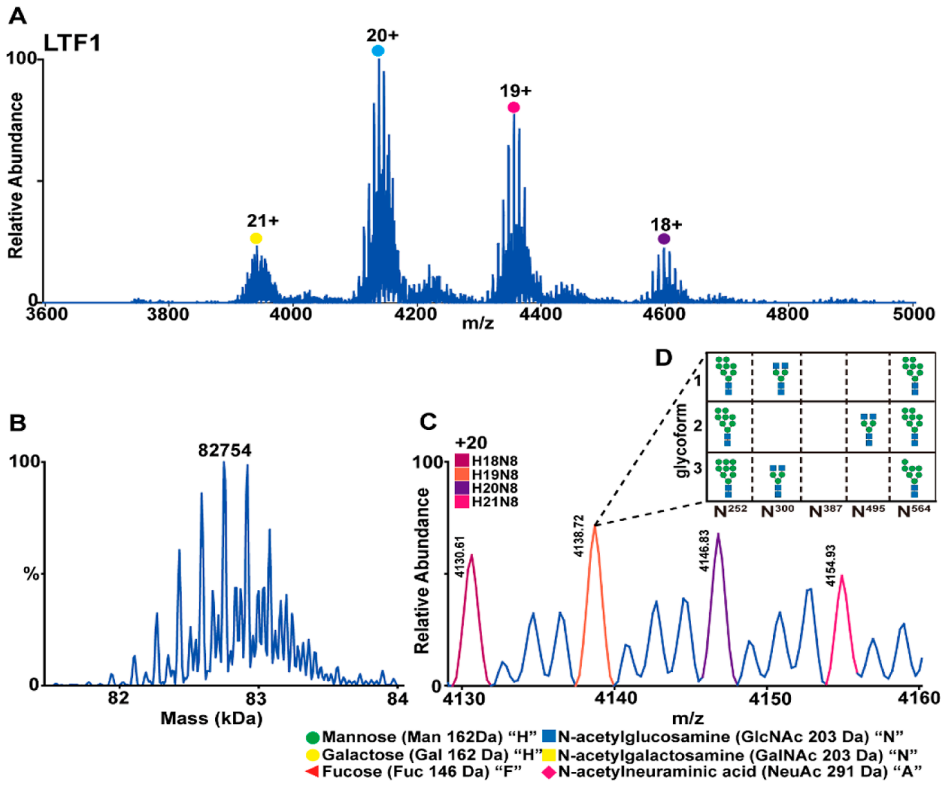

Figure 2. NMS characterization of LTF1 (A), MW measurement after deconvolution (B), distribution of different N-glycans in LTF1 (C), and compositions of the three site-specific glycan combinations matching the most abundant LTF1 form (m/z 4138.72) in nMS (D).

capillary (1.0 mm o.d. and 0.58 mm i.d.) by using a microcapillary puller with an infrared laser (model P-2000). Furthermore, SEC was coupled with nMS,[42] and quantitative analysis was achieved by using the extracted LTF peak intensity in SEC−nMS analysis.

2.6. SDS-PAGE Analysis. SDS-PAGE analysis was carried out to monitor the formation of LTF dimers. LTF sample solution was dissolved in 25 mM Tris HCl (pH = 7.5) solution to achieve a final concentration of 10 μM, and then 10 μL of 5 × SDS-PAGE loading buffer (CWBIO, China) was added and heated at 100 °C for 5 min. Colored prestained standard protein (NCM, China) was included as a marker for electrophoresis. Subsequently, the gel was immersed in M5 HiPer Supermicroscale Protein Stain (Mei5bio, China) for staining and decolorized with deionized water. The gray scale value of the band was determined using ImageJ software (https://imagej.nih.gov/ij/download.html).

2.7. Antimicrobial Activity Assay. The agar diffusion assay was performed by using a modified agar diffusion method.[43] Bacterial suspensions were uniformly plated on the agar medium (10^6 CFU/mL). Drilled wells and a certain concentration of LTF aqueous solutions were added into the well (20 μL/well). Chlorhexidine aqueous solution (2 MIC, 9.35 μg/mL) and sterile water were utilized as the positive and negative controls, respectively. The plate was incubated at 37 °C for 24 h in an incubator. Subsequently, the diameters of bacterial growth inhibition zones were measured.

2.8. Statistical Analysis. The experiments were conducted three times, and the statistical analysis was performed by using EXCEL. A two-sample t-test was employed at a significance level of $p < 0.05$ to evaluate the difference.

3. RESULTS AND DISCUSSION

3.1. nMS Characterization of the LTF Heterogeneity. To demonstrate the feasibility and benefits of the nMS approach, we introduced the nondenaturing LTF1 into the MS gas phase via nESI.[44] The LTF1 mass peaks were distributed in the mass range from 3600 to 5000 m/z with high purity, corresponding to 21+ to 18+ charge states, and the 20+ charged form was the most abundant one (Figure 2A). The clear and narrow distribution of charge states indicated the high sample purity, and the compact structure of LTF1 could be well retained during the transfer from solution to the gas phase by nESI.[27] After deconvolution, the main MW of LTF1 was 82,754 Da (Figure 2B). Compared to the LTF theoretical MW 78,056 Da (Uniprot no. p24627), the mass difference of 4698 Da might account for the modified glycans. Based on the mass difference matching,[45] the total glycans in the dominant LTF1 form (m/z 4138.72) might be H19N8 (Figure 2C). The four adjacent mass peaks exhibit a mass difference of 162 Da, implying one Man or Gal monosaccharide difference. Further, many low-abundance mass peaks are also observed in the nMS spectrum of LTF1, indicating its high glycosylation heterogeneity. In LTF1, the total glycan composition of different forms is mainly H18N8 to H21N8. In contrast, the mass peaks of denatured LTF1 were found to be widely distributed from 1000 to 3000 m/z with much higher charge states ranging from 62+ to 46+ in conventional denatured ESI-MS analysis (Figure S1). The high charge states demonstrated that the LTF1 structure was largely unfolded and disrupted during the denatured ESI process.[46] Moreover, due to the significant peak overlaps among different charge states, the accurate MW determination and purity evaluation of LTF were quite challenging. Overall, the nMS strategy was more suitable for the characterization of purity, MW, conformation maintenance, and glycosylation heterogeneity of LTF.

Then, we further performed glycoproteomic analysis to determine the site-specific N-glycans and their relative occupancy on LTF1. The sequences and N-glycans were identified by HCD and EThcD fragmentation patterns, respectively. According to the Uniprot database, LTF1 has 5

https://doi.org/10.1021/acs.jafc.3c08860
J. Agric. Food Chem. 2024, 72, 10089−10096

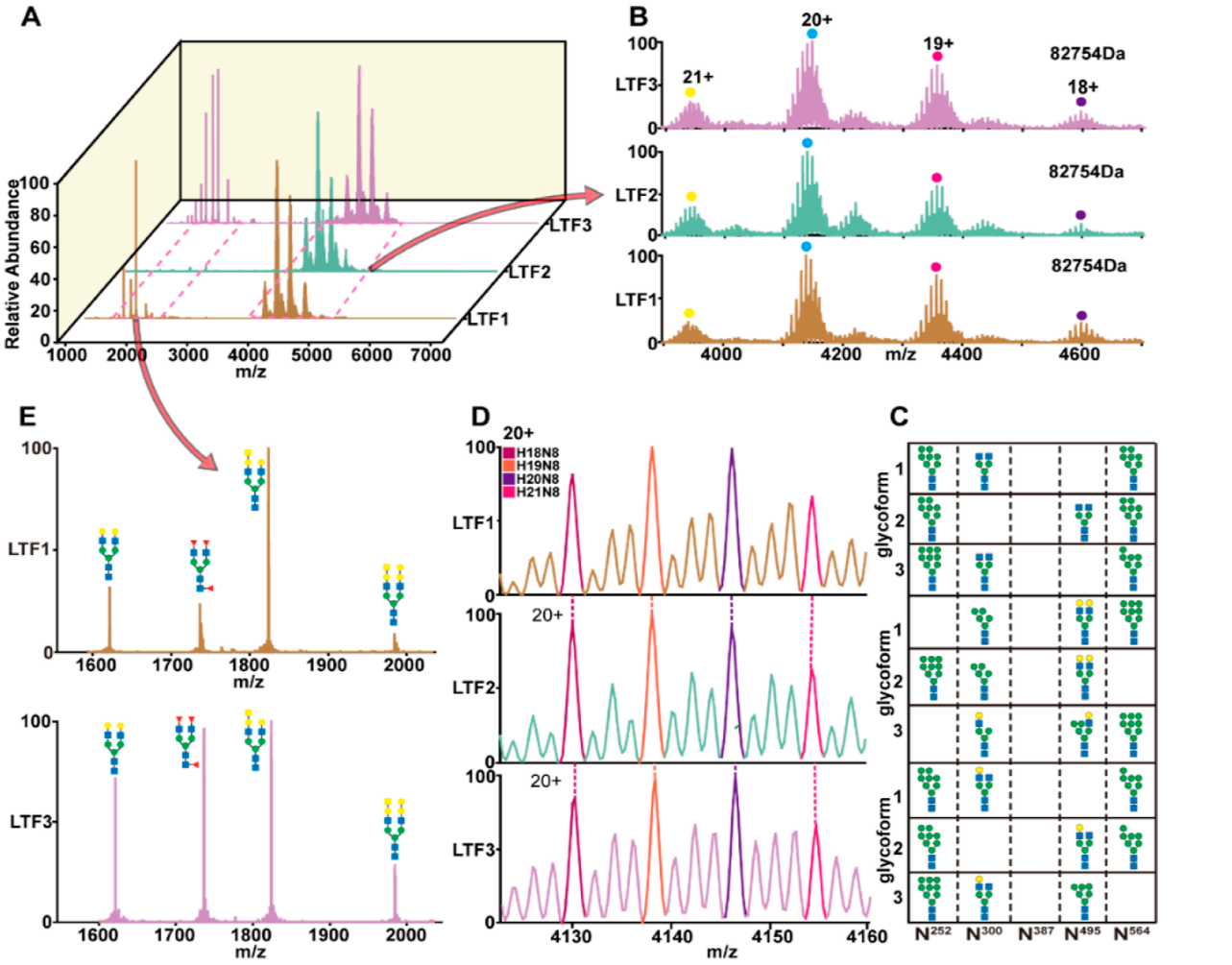

Figure 3. NMS spectra of LTF1, LTF2, and LTF3 (A); the charge state distributions and proteoform patterns (B); the combinations of top 3 potential glycan structures of the dominant LTF forms in nMS (C); the distribution of different N-glycan types (D); and the potential structures of degraded glycans from LTF1 and LTF3 (E).

potential N-glycosylation sites: N252, N300, N387, N495, and N564. In our results, 4 N-glycosylation sites (N252, N300, N495, and N564) and 32 N-glycans were confidently identified (Table S1 and Figures S2A, S4, and S5). N252 and N564 were all modified by the high mannose-type N-glycans, and their N-glycans were relatively conserved with dominant 1−2 N-glycan structures. In contrast, the N-glycans on N300 and N495 exhibited huge microheterogeneity. For N300, which was mainly modified by the complex-type N-glycans, sialylated structures were common, accounting for about 40.6%, and 4 core-fucosylated structures were also observed (Figures S2 and S4). N495 was mostly modified by the hybrid-type N-glycans and a small part by the high mannose-type N-glycans with almost no sialylation and fucosylation. Further, the glycoproteomic analysis results were utilized to match the site-specific N-glycans in the nMS spectrum. For the most abundant LTF1 form in nMS, we derived the most probable 3 N-glycan combinations (Figure 2D): H8N2, H3N4, and H8N2 on N252, N300, and N564 sites; H8N2, H3N4, and H8N2 on N252, N495, and N564 sites; or H9N2, H3N4, and H7N2 on N252, N300, and N564 sites, respectively.

3.2. nMS Analysis of LTF Samples from Different Milk Sources. To evaluate the influence of the milk source on LTF quality at the molecular level, we compared the three bovine LTF samples from different sources (LTF1, 2, and 3) by using nMS (Figure 3A). Similar to LTF1, the mass peaks of LTF2 and LTF3 were also located in the range of 3500 to 5000 m/z, corresponding to charge states from 21+ to 18+, with similar proteoform distribution patterns in each charge state (Figure 3B). After deconvolution, the main MWs of LTF1, 2, and 3 were all about 82 kDa, indicating the high similarity in sequence, glycosylation, and conformation of these three different LTF samples at the molecular level.

We further digested the three LTF samples and sequenced the peptides via bottom-up proteomics, and 90% sequence coverages were obtained for all three samples (Figure S3). Glycoproteomic analyses were also performed to profile the site-specific N-glycans of LTF2 and LTF3 (Table S1 and Figure S2). LTF2 and LTF3 identified 35 and 33 N-glycans at 4 N-glycosylation sites, respectively (Figure S2B,C). Similar to LTF1, N252 and N564 were all modified by the high mannose-type N-glycans, which were relatively conserved. N300 and N495 contained fucosylated and sialylated N-glycans, which were manually verified by MS2 spectra (Figure S4). Overall, the three LTF samples exhibited identical glycosylation sites including N252, N300, N495, and N564. The N-glycans and occupancy of LTF2 and LTF3 were similar to LTF1 at N252 and N564 but greatly different among each

https://doi.org/10.1021/acs.jafc.3c08860
J. Agric. Food Chem. 2024, 72, 10089−10096

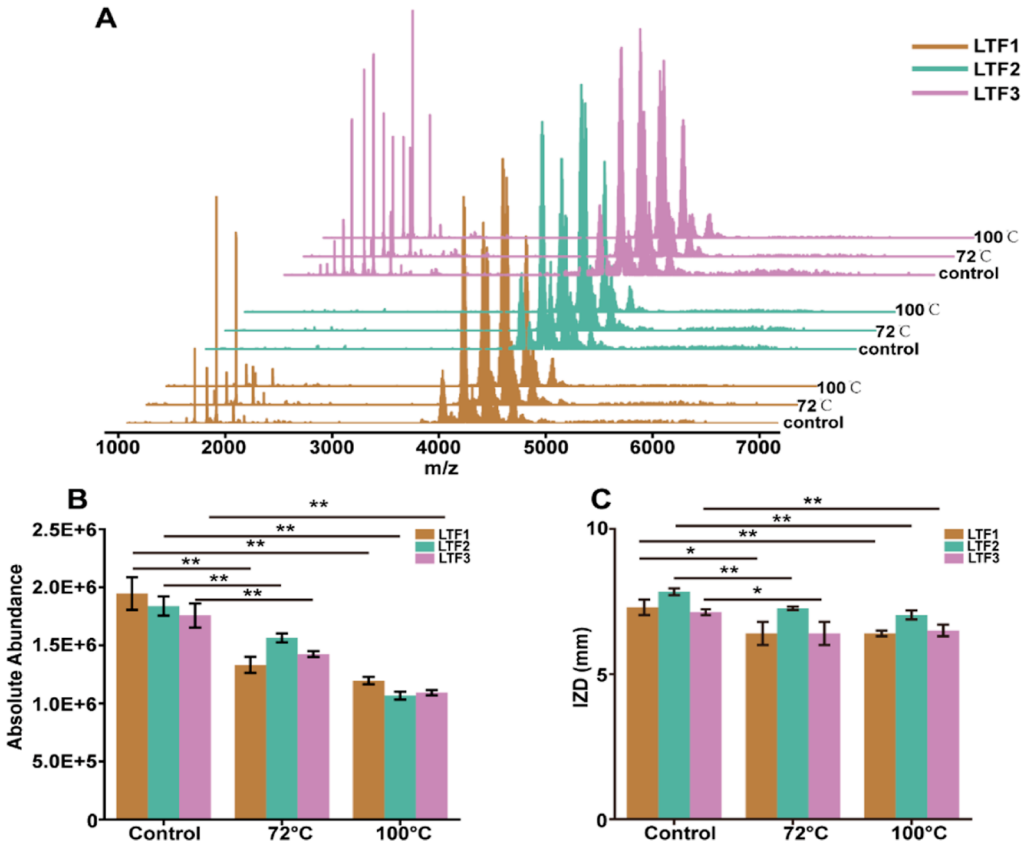

Figure 4. NMS spectra of LTF1, LTF2, and LTF3 under transient high-temperature treatment conditions of 72 °C for 15 s and 100 °C for 10 s (A); quantitative peak intensities (B) and antimicrobial activities (C) of LTF1, LTF2, and LTF3 under different treatments. The three LTF samples against *E. coli* were measured at 50 mg/mL. * when $p < 0.05$ and ** when $p < 0.01$.

other at N300 and N495. The results indicated the differences in the composition of N-glycans among different LTF samples (Figure S2), which may potentially affect the quality of LTF because glycosylation modification is intricately linked with its functional activity.[47]

Next, the site-specific N-glycans obtained from the glycoproteomic analysis were matched with the MW of total glycans (4698 Da) in the nMS results to annotate the N-glycosylation of LTF2 and LTF3. By combining the glycan compositions with relatively high occupancy on each site, we listed the top 3 potential combinations (Figure 3C). The potential N-glycan compositions of LTF2 are H5N2, H5N4, and H9N2 or H4N3, H6N3, and H9N2 on the N300, N495, and N564 sites and H9N2, H5N2, and H5N4 on the N252, N300, and N495 sites, respectively. The potential N-glycan compositions of LTF3 are H8N2, H4N4, and H7N2 on the N252, N300, and N564 sites; H8N2, H4N4, and H7N2 on the N252, N495, and N564 sites; or H9N2, H4N4, and H6N2 on the N252, N300, and N495 sites, respectively. The difference is in the degree of glycan branching and glycoforms. The degree of glycan branching consists of double or triple antennas. The most abundant glycoform is the high-mannose type. Furthermore, the extended double strand is modified with one or two Gal, first extended with GlcNAc and then attached to Gal. No sialylated structure is observed, as is the modification of the fucosylation. Although the three LTF samples matched different glycosylation patterns, the total glycan compositions of the main forms were all H19N8. Further, the total glycan composition of different forms on LTF1, LTF2, and LTF3 are all H18N8 to H21N8 (Figure 3D).

In addition to the mass peaks of proteoforms, some low-MW peaks were also observed in the range of 1000−2000 m/z in nMS, which exhibited significant differences among the three LTF samples. Matching these peaks with the MWs of glycans, we confirmed that these low-MW peaks resulted from the release of glycan chains from LTF (Figure 3E). Interestingly, glycan chains were detected in LTF1 and LTF3 but not in LTF2. Overall, nMS and glycoproteomic analysis can successfully compare the glycosylation modifications in detail of different LTF samples as well as the glycan degradation during the processing or storage processes.

3.3. Effects of Heat Treatment on LTF. Since LTF is frequently used as an active additive in functional foods, it is important to evaluate its active conformation and thermal stability when used as bioactive ingredients. Nevertheless, thermal processing, a necessary step to transform LTF from raw material to product, may cause alterations in its conformation and activity, thus affecting the anticipated bioactivity of LTF. Pasteurization and ultrahigh-temperature instantaneous sterilization are the most commonly used disinfection methods for liquid milk production.[48] Therefore, we simulated transient high-temperature treatments including 72 °C for 15 s and 100 °C for 10 s to investigate the effects of thermal processing on the LTF conformation and activity.

After heat treatment, the distribution patterns of LTF peaks and charge states were identical to the untreated ones, indicating that the compact structures could be well retained during the transient high-temperature processes (Figures 4A

https://doi.org/10.1021/acs.jafc.3c08860
J. Agric. Food Chem. 2024, 72, 10089−10096

and S6). We further performed SEC−nMS to quantify the intensities of LTF samples under different treatments. Along with the increase in treatment temperature, the peak intensity of LTF samples all exhibited decreasing trends (Figure 4B). In brief, the LTF intensity decreased by about 22 and 40% under 72 and 100 °C treatments, respectively. Therefore, although the compact conformations of LTF can be preserved as shown in nMS, it seems that part of the LTF might be denatured and precipitated during the high-temperature treatment. To further clarify the structural changes of LTF samples before and after heat treatment, we performed deconvolution analysis of the nMS spectra and analyzed the degree of protein aggregation by SDS-PAGE. The results showed that there were peaks around 160 kDa in the three LTF samples before and after heat treatment, which were inferred from the LTF dimers with different glycoforms (Figure S7). The relative abundances of LTF dimers were positively related to the temperature of heat treatment. Similar trends were also observed by using SDS-PAGE. LTF3 might be precipitated under heat treatment (Figure S8 and Table S2). Statistical analysis of the band grayscales of SDS-PAGE by the *t*-test (Table S2) found that the band grayscales of three LTF samples were significantly different after heating (72 and 100 °C).

LTF shows broad-spectrum antimicrobial activity and has a strong inhibitory effect on Gram-negative bacteria *E. coli*. After transient high-temperature treatments, LTF samples still maintained their inhibitory activity. With the increase in treatment temperature, the activity of *E. coli* gradually decreased (Figure 4C); compared with LTF2, the antimicrobial activity of LTF1 and 3 decreased significantly while heated to 100 °C, exhibiting a similar trend to the quantitative results of SEC−nMS.

As LTF is a heat-unstable protein, it is well-known that heat treatment of LTF affects its active structure and biological function. Therefore, the structural stability of LTF is very important for its bioactivity maintenance. Despite significant advancements in quality control for the industrial production of highly active LTF, the structure stability analysis of LTF is still inadequate. Stănciuc et al. applied fluorescence spectroscopy and enzymic hydrolysis to investigate the thermal behavior of LTF.[14] LC strategies including RPLC and SEC are commonly used for LTF quality control in industrial production but cannot provide information about structure and bioactivity. In this study, we demonstrate that the nMS strategy makes it possible to rapidly analyze the purity, conformation stability, and glycosylation heterogeneity of LTF samples, which might greatly promote the quality improvement of active LTF production.

In this study, we developed an nMS and glycoproteomic strategy to characterize the purity, MW, conformation stability, glycosylation heterogeneity, and activity of LTF samples from different milk sources and under different heat treatments. We demonstrated that the LTF samples from different milk sources had high glycosylation heterogeneity. Further, the conformation stability of LTF samples could be feasibly evaluated by using the charge state distribution patterns as well as the quantitative peak intensities in SEC−nMS analysis, which were positively related to their antimicrobial activity. Overall, this nMS strategy shows high sensitivity and reliability to probe the purity, MW, and structural insights of LTF samples at the molecular level, which might be an ideal alternative for the quality control of high-quality LTF samples.

■ ASSOCIATED CONTENT

Supporting Information

The Supporting Information is available free of charge at https://pubs.acs.org/doi/10.1021/acs.jafc.3c08860.

Mass spectra of denatured LTF1; overview of the qualitative and semiquantitative site-specific glycosylation in three LTF samples; sequence coverages of the three LTF samples; manual validation of the MS2 spectra of fucosylated and sialylated glycans retrieved by the gLabel.exe program in two fragmentation modes: HCD and EThcD; manual verification of MS2 spectra retrieved by the gLabel.exe program performed in both fragmentation modes: HCD and EThcD; schematic diagrams of the degraded glycans of LTF1 and LTF3 in the low MW region after 72 °C for 15 s and 100 °C for 10 s heat treatments; MW distribution of three LTF samples after deconvolution; SDS-PAGE analysis of LTF samples under heat treatment with different temperatures; and SDS-PAGE band intensity of LTF dimers under heat treatment (PDF)

Detailed information regarding three LTF samples, including peptide sequences, glycan structures, peak areas, etc. (XLS)

■ AUTHOR INFORMATION

Corresponding Authors

Yan Jin − *CAS Key Laboratory of Separation Sciences for Analytical Chemistry, Dalian Institute of Chemical Physics, Chinese Academy of Sciences, Dalian 116023, China;* orcid.org/0000-0002-3694-9723; Email: yanjin@dicp.ac.cn

Yanxia Qi − *College of Food Science and Engineering, Ocean University of Dalian, Dalian 116023, China;* Email: qiyanxia@dlou.edu.cn

Fangjun Wang − *CAS Key Laboratory of Separation Sciences for Analytical Chemistry, Dalian Institute of Chemical Physics and State Key Laboratory of Molecular Reaction Dynamics, Dalian Institute of Chemical Physics, Chinese Academy of Sciences, Dalian 116023, China; Inner Mongolia National Center of Technology Innovation for Dairy Co. Ltd., Hohhot 010110, China; University of Chinese Academy of Sciences, Beijing 100049, China;* orcid.org/0000-0002-8118-7019; Email: wangfj@dicp.ac.cn

Authors

Yu Mu − *College of Food Science and Engineering, Ocean University of Dalian, Dalian 116023, China; CAS Key Laboratory of Separation Sciences for Analytical Chemistry, Dalian Institute of Chemical Physics, Chinese Academy of Sciences, Dalian 116023, China*

Shan Zhao − *CAS Key Laboratory of Separation Sciences for Analytical Chemistry, Dalian Institute of Chemical Physics and State Key Laboratory of Molecular Reaction Dynamics, Dalian Institute of Chemical Physics, Chinese Academy of Sciences, Dalian 116023, China*

Jing Liu − *CAS Key Laboratory of Separation Sciences for Analytical Chemistry, Dalian Institute of Chemical Physics, Chinese Academy of Sciences, Dalian 116023, China; College of Pharmacy, Dalian Medical University, Dalian 116044, China*

Zheyi Liu − *CAS Key Laboratory of Separation Sciences for Analytical Chemistry, Dalian Institute of Chemical Physics, Chinese Academy of Sciences, Dalian 116023, China*

Jian He − *Inner Mongolia Dairy Technology Research Institute Co., Ltd., Hohhot 010110, China; Inner Mongolia National Center of Technology Innovation for Dairy Co. Ltd., Hohhot 010110, China*

Hongfang Cao − *Inner Mongolia Dairy Technology Research Institute Co., Ltd., Hohhot 010110, China; Inner Mongolia National Center of Technology Innovation for Dairy Co. Ltd., Hohhot 010110, China*

Heng Zhao − *CAS Key Laboratory of Separation Sciences for Analytical Chemistry, Dalian Institute of Chemical Physics and State Key Laboratory of Molecular Reaction Dynamics, Dalian Institute of Chemical Physics, Chinese Academy of Sciences, Dalian 116023, China*

Caiyun Wang − *Inner Mongolia Dairy Technology Research Institute Co., Ltd., Hohhot 010110, China; Inner Mongolia National Center of Technology Innovation for Dairy Co. Ltd., Hohhot 010110, China*

Complete contact information is available at: https://pubs.acs.org/10.1021/acs.jafc.3c08860

Author Contributions

[▽]Y.M. and S.Z. contributed equally.

Notes

The authors declare no competing financial interest.

■ ACKNOWLEDGMENTS

We acknowledge the financial support from the National Natural Science Foundation of China (32088101), the Huhhot Science & Technology Plan (National Dairy Innovation Center, no. 2021-10), the Open Fund of National Center of Technology Innovation for Dairy (no. 2022-Open Fund-14), the Scientific Instrument Developing Project of the Chinese Academy of Sciences (GJJSTD20220001), and the grant from DICP (DICPI202242). The authors acknowledge Prof. Xin-Miao Liang and Prof. Xiu-Ling Li (Dalian Institute of Chemical Physics, Chinese Academy of Sciences) for providing the "click maltose" HILIC material. The authors acknowledge the technological support of the biological mass spectrometry station of Dalian Coherent Light Source.

■ REFERENCES

(1) Conesa, C.; Sánchez, L.; Pérez, M. D.; Calvo, M. A calorimetric study of thermal denaturation of recombinant human lactoferrin from rice. *J. Agric. Food Chem.* **2007**, *55* (12), 4848−4853.

(2) Redwan, E. M.; Uversky, V. N.; El-Fakharany, E. M.; Al-Mehdar, H. Potential lactoferrin activity against pathogenic viruses. *C. R. Biol.* **2014**, *337* (10), 581−595.

(3) Mayeur, S.; Spahis, S.; Pouliot, Y.; Levy, E. Lactoferrin, a pleiotropic protein in health and disease. *Antioxid. Redox Signaling* **2016**, *24* (14), 813−836.

(4) Wang, B.; Timilsena, Y. P.; Blanch, E.; Adhikari, B. Lactoferrin: Structure, function, denaturation and digestion. *Crit. Rev. Food Sci. Nutr.* **2019**, *59* (4), 580−596.

(5) Artym, J.; Zimecki, M. Antimicrobial and prebiotic activity of lactoferrin in the female reproductive tract: A comprehensive review. *Biomedicines* **2021**, *9* (12), 1940.

(6) Bielecka, M.; Cichosz, G.; Czeczot, H. Antioxidant, antimicrobial and anticarcinogenic activities of bovine milk proteins and their hydrolysates - a review. *Int. Dairy J.* **2022**, *127*, 105208.

(7) Valk-Weeber, R. L.; Eshuis-de Ruiter, T.; Dijkhuizen, L.; van Leeuwen, S. S. Dynamic temporal variations in bovine lactoferrin glycan structures. *J. Agric. Food Chem.* **2020**, *68* (2), 549−560.

(8) Geagea, H.; Gomaa, A.; Remondetto, G.; Moineau, S.; Subirade, M. Molecular structure of lactoferrin influences the thermal resistance of lactococcal phages. *J. Agric. Food Chem.* **2017**, *65* (10), 2214−2221.

(9) Li, W.; Liu, B.; Lin, Y.; Xue, P.; Lu, Y.; Song, S.; Li, Y.; Szeto, I. M.; Ren, F.; Guo, H. The application of lactoferrin in infant formula: The past, present and future. *Crit. Rev. Food Sci. Nutr.* **2022**, 1−20.

(10) Somm, E.; Larvaron, P.; van de Looij, Y.; Toulotte, A.; Chatagner, A.; Faure, M.; Métairon, S.; Mansourian, R.; Raymond, F.; Gruetter, R.; Wang, B.; Sizonenko, S. V.; Hüppi, P. S. Protective effects of maternal nutritional supplementation with lactoferrin on growth and brain metabolism. *Pediatr. Res.* **2014**, *75* (1), 51−61.

(11) Tsuda, H.; Sekine, K.; Ushida, Y.; Kuhara, T.; Takasuka, N.; Iigo, M.; Han, B. S.; Moore, M. A. Milk and dairy products in cancer prevention: Focus on bovine lactoferrin. *Mutat. Res. Rev. Mutat. Res.* **2000**, *462* (2−3), 227−233.

(12) Wormald, M. R.; Petrescu, A. J.; Pao, Y.-L.; Glithero, A.; Elliott, T.; Dwek, R. A. Conformational studies of oligosaccharides and glycopeptides: Complementarity of nmr, x-ray crystallography, and molecular modelling. *Chem. Rev.* **2002**, *102* (2), 371−386.

(13) Baker, E. N.; Baker, H. M. A structural framework for understanding the multifunctional character of lactoferrin. *Biochimie* **2009**, *91* (1), 3−10.

(14) Stănciuc, N.; Aprodu, I.; Râpeanu, G.; van der Plancken, I.; Bahrim, G.; Hendrickx, M. Analysis of the thermally induced structural changes of bovine lactoferrin. *J. Agric. Food Chem.* **2013**, *61* (9), 2234−2243.

(15) Goulding, D. A.; O'Regan, J.; Bovetto, L.; O'Brien, N. M.; O'Mahony, J. A. Influence of thermal processing on the physicochemical properties of bovine lactoferrin. *Int. Dairy J.* **2021**, *119*, 105001.

(16) Fan, F.; Liu, M.; Shi, P.; Xu, S.; Lu, W.; Du, M. Effects of thermal treatment on the physicochemical properties and osteogenic activity of lactoferrin. *J. Food Process. Preserv.* **2019**, *43* (9), No. e14068.

(17) Brisson, G.; Britten, M.; Pouliot, Y. Heat-induced aggregation of bovine lactoferrin at neutral ph: Effect of iron saturation. *Int. Dairy J.* **2007**, *17* (6), 617−624.

(18) Franco, I.; Castillo, E.; Pérez, M.; Calvo, M.; Sánchez, L. Effect of bovine lactoferrin addition to milk in yogurt manufacturing. *J. Dairy Sci.* **2010**, *93* (10), 4480−4489.

(19) Pochet, S.; Arnould, C.; Debournoux, P.; Flament, J.; Rolet-Répécaud, O.; Beuvier, E. A simple micro-batch ion-exchange resin extraction method coupled with reverse-phase hplc (mbre-hplc) to quantify lactoferrin in raw and heat-treated bovine milk. *Food Chem.* **2018**, *259*, 36−45.

(20) Drackova, M.; Borkovcova, I.; Janstova, B.; Naiserova, M.; Pridalova, H.; Navratilova, P.; Vorlova, L. Determination of lactoferrin in goat milk by hplc method. *Czech J. Food Sci.* **2009**, *27* (Special Issue 1), S102−S104.

(21) Yao, X.; Bunt, C.; Cornish, J.; Quek, S.-Y.; Wen, J. Improved rp-hplc method for determination of bovine lactoferrin and its proteolytic degradation in simulated gastrointestinal fluids. *Biomed. Chromatogr.* **2013**, *27* (2), 197−202.

(22) Tsakali, E.; Chatzilazarou, A.; Houhoula, D.; Koulouris, S.; Tsaknis, J.; Van Impe, J. A rapid hplc method for the determination of lactoferrin in milk of various species. *J. Dairy Res.* **2019**, *86* (2), 238−241.

(23) Staub, A.; Guillarme, D.; Schappler, J.; Veuthey, J.-L.; Rudaz, S. Intact protein analysis in the biopharmaceutical field. *J. Pharm. Biomed. Anal.* **2011**, *55* (4), 810−822.

(24) Bolla, J. R.; Sauer, J. B.; Wu, D.; Mehmood, S.; Allison, T. M.; Robinson, C. V. Direct observation of the influence of cardiolipin and antibiotics on lipid ii binding to murj. *Nat. Chem.* **2018**, *10* (3), 363−371.

(25) Chen, Z. A.; Rappsilber, J. Quantitative cross-linking/mass spectrometry to elucidate structural changes in proteins and their complexes. *Nat. Protoc.* **2019**, *14* (1), 171−201.
(26) Mehaffey, M. R.; Schardon, C. L.; Novelli, E. T.; Cammarata, M. B.; Webb, L. J.; Fast, W.; Brodbelt, J. S. Investigation of gtp-dependent dimerization of g12x k-ras variants using ultraviolet photodissociation mass spectrometry. *Chem. Sci.* **2019**, *10* (34), 8025−8034.
(27) Leney, A. C.; Heck, A. J. R. Native mass spectrometry: What is in the name? *J. Am. Soc. Mass Spectrom.* **2017**, *28* (1), 5−13.
(28) Zhang, W. X.; Liu, Z. Y.; Zhou, Y.; Lai, C.; Sun, B.; He, M.; Zhai, Z.; Wang, J.; Wang, Q.; Wang, X.; Wang, F.; Pan, Y. Elucidating the molecular mechanisms of perfluorooctanoic acid-serum protein interactions by structural mass spectrometry. *Chemosphere* **2022**, *291*, 132945.
(29) Bai, Y.; Liu, Z.; Li, Y.; Zhao, H.; Lai, C.; Zhao, S.; Chen, K.; Luo, C.; Yang, X.; Wang, F. Structural mass spectrometry probes the inhibitor-induced allosteric activation of cdk12/cdk13-cyclin k dissociation. *J. Am. Chem. Soc.* **2023**, *145* (21), 11477−11481.
(30) Liu, Z.; Chen, X.; Yang, S.; Tian, R.; Wang, F. Integrated mass spectrometry strategy for functional protein complex discovery and structural characterization. *Curr. Opin. Chem. Biol.* **2023**, *74*, 102305.
(31) Tamara, S.; den Boer, M. A.; Heck, A. J. R. High-resolution native mass spectrometry. *Chem. Rev.* **2022**, *122* (8), 7269−7326.
(32) Yen, H.-Y.; Liko, I.; Song, W.; Kapoor, P.; Almeida, F.; Toporowska, J.; Gherbi, K.; Hopper, J. T. S.; Charlton, S. J.; Politis, A.; Sansom, M. S. P.; Jazayeri, A.; Robinson, C. V. Mass spectrometry captures biased signalling and allosteric modulation of a g-protein-coupled receptor. *Nat. Chem.* **2022**, *14* (12), 1375−1382.
(33) Chen, S.; Getter, T.; Salom, D.; Wu, D.; Quetschlich, D.; Chorev, D. S.; Palczewski, K.; Robinson, C. V. Capturing a rhodopsin receptor signalling cascade across a native membrane. *Nature* **2022**, *604* (7905), 384−390.
(34) Heck, A. J. R. Native mass spectrometry: A bridge between interactomics and structural biology. *Nat. Methods* **2008**, *5* (11), 927−933.
(35) Zhou, L.; Liu, Z.; Guo, Y.; Liu, S.; Zhao, H.; Zhao, S.; Xiao, C.; Feng, S.; Yang, X.; Wang, F. Ultraviolet photodissociation reveals the molecular mechanism of crown ether microsolvation effect on the gas-phase native-like protein structure. *J. Am. Chem. Soc.* **2023**, *145* (2), 1285−1291.
(36) Rosati, S.; Yang, Y.; Barendregt, A.; Heck, A. J. R. Detailed mass analysis of structural heterogeneity in monoclonal antibodies using native mass spectrometry. *Nat. Protoc.* **2014**, *9* (4), 967−976.
(37) Lin, Y.-H.; Franc, V.; Heck, A. J. R. Similar albeit not the same: In-depth analysis of proteoforms of human serum, bovine serum, and recombinant human fetuin. *J. Proteome Res.* **2018**, *17* (8), 2861−2869.
(38) Rolland, A. D.; Prell, J. S. Approaches to heterogeneity in native mass spectrometry. *Chem. Rev.* **2022**, *122* (8), 7909−7951.
(39) Yu, L.; Li, X.; Guo, Z.; Zhang, X.; Liang, X. Hydrophilic interaction chromatography based enrichment of glycopeptides by using click maltose: A matrix with high selectivity and glycosylation heterogeneity coverage. *Chem.—Eur. J.* **2009**, *15* (46), 12618−12626.
(40) Liu, J.; Lv, J.; Liu, Z. Y.; Fang, Z.; Lai, C.; Zhao, S.; Ye, M.; Wang, F. Enhanced interfacial h-bond networks promote glycan-glycan recognition and interaction. *ACS Appl. Mater. Interfaces* **2023**, *15* (14), 17592−17600.
(41) Zeng, W.-F.; Cao, W.-Q.; Liu, M.-Q.; He, S.-M.; Yang, P.-Y. Precise, fast and comprehensive analysis of intact glycopeptides and modified glycans with pglyco3. *Nat. Methods* **2021**, *18* (12), 1515−1523.
(42) Haberger, M.; Leiss, M.; Heidenreich, A.-K.; Pester, O.; Hafenmair, G.; Hook, M.; Bonnington, L.; Wegele, H.; Haindl, M.; Reusch, D.; Bulau, P. Rapid characterization of biotherapeutic proteins by size-exclusion chromatography coupled to native mass spectrometry. *mAbs* **2016**, *8* (2), 331−339.
(43) Zhao, Q.; Shi, Y.; Wang, X.; Huang, A. Characterization of a novel antimicrobial peptide from buffalo casein hydrolysate based on live bacteria adsorption. *J. Dairy Sci.* **2020**, *103* (12), 11116−11128.
(44) Kafader, J. O.; Melani, R. D.; Schachner, L. F.; Ives, A. N.; Patrie, S. M.; Kelleher, N. L.; Compton, P. D. Native vs denatured: An in depth investigation of charge state and isotope distributions. *J. Am. Soc. Mass Spectrom.* **2020**, *31* (3), 574−581.
(45) Chen, S.; Wu, D.; Robinson, C. V.; Struwe, W. B. Native mass spectrometry meets glycomics: Resolving structural detail and occupancy of glycans on intact glycoproteins. *Anal. Chem.* **2021**, *93* (30), 10435−10443.
(46) Krusemark, C. J.; Frey, B. L.; Belshaw, P. J.; Smith, L. M. Modifying the charge state distribution of proteins in electrospray ionization mass spectrometry by chemical derivatization. *J. Am. Soc. Mass Spectrom.* **2009**, *20* (9), 1617−1625.
(47) Karav, S. Selective deglycosylation of lactoferrin to understand glycans' contribution to antimicrobial activity of lactoferrin. *Cell. Mol. Biol.* **2018**, *64* (9), 52−57.
(48) Ritota, M.; Di Costanzo, M. G.; Mattera, M.; Manzi, P. New trends for the evaluation of heat treatments of milk. *J. Anal. Methods Chem.* **2017**, *2017*, 1−12.

https://doi.org/10.1021/acs.jafc.3c08860
J. Agric. Food Chem. 2024, 72, 10089−10096